Rev.Adv.Mater.Sci. 26(2010) 30-42

POLYMER LIGHT EMITTING DIODES - A REVIEW ON MATERIALS AND TECHNIQUES

Shahul Hameed[1], P. Predeep[2] and M.R.Baiju[3]

[1]Department of Electronics and Communication Engineering. TKM College of Engineering, Kollam, Kerala, India
[2]Unconventional Electronics and Photonics Laboratory, National Institute of Technology, Calicut, Kerala, India
[3]Department of Electronics and Communication Engineering, College of Engineering Trivandrum, Kerala, India

Received: February 14, 2010

Abstract. Polymer Light Emitting Diodes, the most promising name in the field of display technology has received tremendous attention from various research groups. Being an interdisciplinary area of research, there has been challenging experiments on material science, device physics and chemistry of this organic display. This review unveils the development of PLEDs from its inception, bringing out important milestones in the materials used and phenomenal variations observed. Starting from the classical single layer device with MEH-PPV as emissive layer, multilayer devices, use of polymer blends, incorporation of nano particles and electro phosphorescent devices are discussed. Attempts have been made to shed light into adoption of alternate design strategies, thickness dependence changes, impedance behavior and the degradation property of the device.

1. INTRODUCTION

Polymer Light Emitting Diodes (PLED) are best suited for large array of displays due to easy processing and mechanical flexibility. Ever since the advent of PLED was reported [1], there has been an unending thrust among researchers on experimenting with many newer materials having electroluminescent property. Various research groups across the world trying with newer materials and technologies report exciting results and bring out tremendous changes in robustness and life of the device. The polymer LED is a dual carrier injection device. The electrons are injected from cathode to the Lowest Unoccupied Molecular Orbital (LUMO) of the polymer and holes are injected from anode to the Highest Occupied Molecular Orbital (HOMO) of conducting polymer and they recombine radiatively within the polymer to give off light. The injection occurs due to tunneling and thermionic emission.

On the way to enhance the efficiency and reliability of the device, researchers are involved in trying different kinds of electrodes and inserting more layers between electrodes. Replacement of anode material, Indium Tin Oxide (ITO) due to its degradation properties, effective enhancement of conductivity of hole transport layers, use of different cathode metals and emissive materials so as to remove impediments in work function, trying with nano particles of component layers *etc*. are the ways to upgrade the performance of the device. In this paper, we attempt to shed light into the device organization, criteria of material selection for high throughputs, use of different materials as emissive layers, performance of hetero layer devices, phenomenal changes due to thickness variations and the impact of material degradation in its electrical and spectral output.

Corresponding author: Shahul Hameed, e-mail: talk2shahu@gmail.com

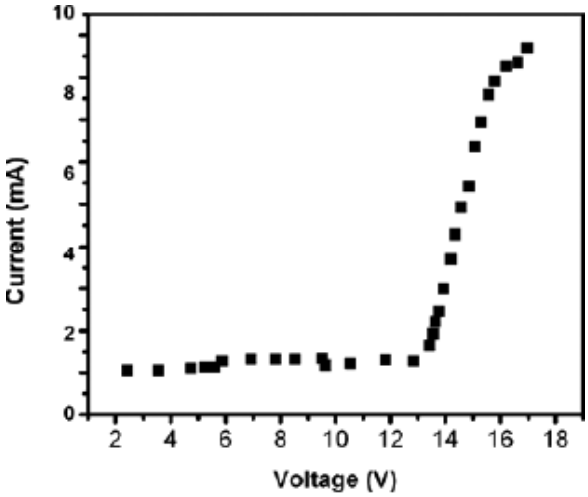

Fig. 1. *I-V* Characteristics of PLED reported in [1].

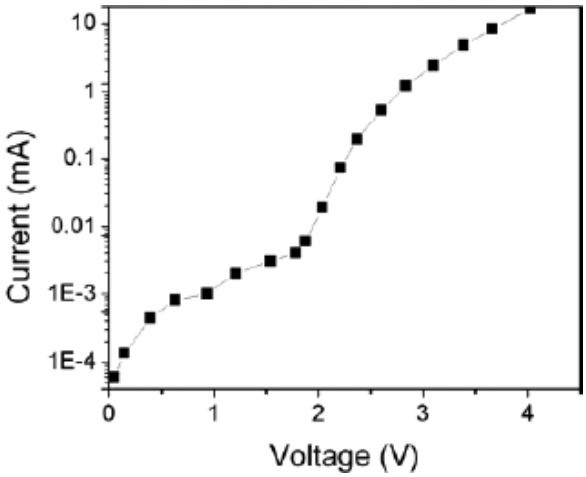

Fig. 2. *V-I* Characteristics of PLED reported in [3].

2. POLYMER LIGHT EMITTING DIODES-SINGLE AND DOUBLE LAYER DEVICES

2.1. MEH-PPV based devices

J. H. Burroughes [1] *et al*. had first fabricated the PLED by using conjugated polymers in 1990. Conjugated polymers are organic semiconductors, semiconducting behavior being associated with π molecular orbitals delocalized along the polymer chain. Possibility of processing to form robust and flexible structure makes them suitable for display arrays

On electronic excitation, injection of electrons and holes on the conjugated chain can lead to a self localized excited state which can decay radiatively. Poly (p-phenylene vinylene) (PPV) prepared by way of a solution precursor was used as the active element in LEDs, with the device configuration ITO anode)/PPV/Ca(cathode). The I-V characteristics (Fig. 1) shows a threshold of charge injection of around 14 V and a high turn on voltage making very high power consumption.

Later, flexible PLED by spin coating a thin layer of poly aniline onto a sheet of poly ethylene terephthalate, Poly (2-methoxy, 5-(2-ethylhexoxy)-1, 4-phenylene-vinylene (MEH- PPV) used as emissive polymer, with calcium cathode [2] was devised. Calcium was deposited by vacuum evaporation and the polymer layer by spin coating. The robust and highly twistable device had shown a turn on voltage at 1.8 V and orange yellow luminescence at 600 nm.

Instead of single layer of ITO, a bilayer of ITO and PEDOT-PSS is used as anode, calcium cathode and MEH-PPV as conducting polymer [3] where PEDOT acts as a hole transport layer. The fabrication of the device was through spin casting of PEDOT and MEH-PPV and this category of device exhibits current and light turn on below 2 V as shown in Fig. 2.

2.2. Multilayer PPV devices

Instead of single layer devices using PPV, there has been a series of experiments carried out with multiple layers where several layers are applied to obtain optimal charge injection, transport and light emission [4,5]. The effect of Li doping in PPV based PLEDs- i.e. between PEDOT-PSS layer and reactive cathode, thin Li layer (1 Å) or a layer of P14NHP of (50 Å) thickness has been added and the performance study of the device shows better results [6]. The devices fabricated are ITO-PEDOT-PPV-Al (Type I), ITO-PEDOT-PPV-Li-Al (Type II), ITO-PEDOT-PPV-P14NHP-Al (Type III) and ITO-PEDOT-PPV-P14NHP-Li-Al (Type IV). Poly (2,5-diheptyl 1-1, 4-phenylene-alt-1,4-naphthylene)- P14NHP is a strictly alternating copolymer with naphthylene and substituted phenylene group in the repeater unit whose electronic structure was included in a previous study [7]. The performances of the above devices are tabulated in Table 1.

There are a number of polyphenylene type emissive materials suitable to be used in multilayer structures of PLED [8]**.** By embedding hole transporting materials (HTLs) in a cross-linked polymer matrix, the improvement in total luminance and external quantum efficiency were demonstrated in multilayer device [9].

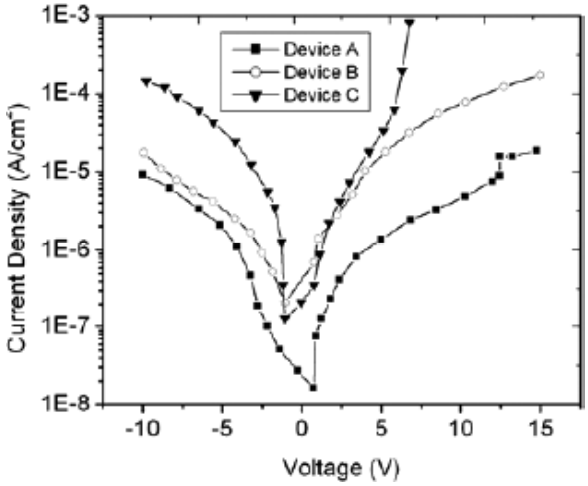

Fig. 3. *J-V* Characteristics of Devices *A*, *B,* and *C* reported in [12].

2.3. Use of polymer blends

Oxadiazole derivatives are used as electron transport layer to provide a balanced injection of charge carriers [10]. In fact, oxadiazole is blended with MEH-PPV, in which electrical conduction is dominated by holes. In making devices with oxadiazole derivatives, two approaches were followed-devices with mixed layer of MEH-PPV + 20% PPyD and a bi layer MEH-PPV/PPyD [11]. The blended one forms a single layer which was characterized for polymer layer thickness ranging from 110 nm to 260 nm. For the device having minimum thickness, turn on voltage is 12 V which is bit higher side whereas the external quantum efficiency of the blended layer device is less than that of the dual layer device.

Different methods of spin casting of MEH-PPV and Cyano Polyphenylene Vinylene (CN-PPV) to form PLEDs principally to asses the degree of intermixing at the interface and its impact on electrical characteristics of the diodes were investigated by Tripathi *et al*. [12]. By using impedance spectroscopy, the impact of intermixing as electrical properties of spin cast heterostructures formed by depositing CN-PPV and MEH-PPV was evaluated.

The extent of coverage of CNPPV prior to its spin coating was varied by three different methods: (A) the MEH-PPV layer was removed to create a valley over a sufficient area (1.5×5 cm^2), in the middle of the substrate, and then the CN-PPV solution 'as spread gently in the valley and then spin coated; (B) the CNPPV solution was spread in the middle of the MEHPPV layer and then spin coated; (C) the CN-PPV solution was spread over the whole layer of

Table 1. Performance of the four types of devices [7].

Device	Turn OnVolt, V	Max. Eff. (cd/A)	Voltage, V	Max. Light (cd/m^2)
Type I	5.7	0.004	11.4	18.9
Type II	3.9	0.025	6.0	40.2
Type III	4.5	0.13	11.0	92.7
Type IV	4.3	0.29	10.4	133

MEH-PPV and then spin coated. The I-V characteristics of three devices made from one of these emissive materials is shown in Fig. 3. Clearly the device C is the leakiest in reverse bias and shows a large jump at about 5 V in forward bias corresponding to a trap filled limit voltage. The intermixing of the two layers in the green state seems to produce a large concentration defect states leading to this jump in forward bias current. In contrast, the device A, where least mixing is expected, does show existence of resistive bi layer in the structure. The *I-V* characteristics of sample B, where mixing is expected to be moderate, shows *I-V* curves typically expected of a hetero structure PLED, with leakage current being intermediate to the case of other two samples. The turn on voltage is approximately similar in all the three cases and lies in the range of 2.8-3 V.

Focusing on increasing the conductivity of PEDOT-PSS for the overall upgradation of PLEDs has gained momentum from various research groups. It include blending with polar host polymers like poly (vinyl pyrrolidone) [13] and electrochemical polymerization and subsequent doping [14]. In such cases, increase in conductivity is accompanied by decrease in optical transmittance. The surface sheet resistance of conducting films of glycerol doped PEDOT-PSS is largely dependent on annealing temperatures. Kim *et al*. [15] reported the performance of the device having G: PEDOT-PSS (150 nm) as anode, N-N'-bis (baphthalene-1-yl)-N-N'-bis (phenyl) benzidine (NPB-50 nm) as hole transport layer, Tris (8-hydroxyquinolinato) aluminium (AlQ3) (70 nm) as electron transport layer and Mg:Ag (160 nm) at 18:1 ratio as cathode. The PEDOT has kept at different baking temperatures of 130, 150, 170, and 190 °C and current density, luminance and luminous efficiency are found to be higher at higher temperatures. Better performance is reported for devices which have been baked for

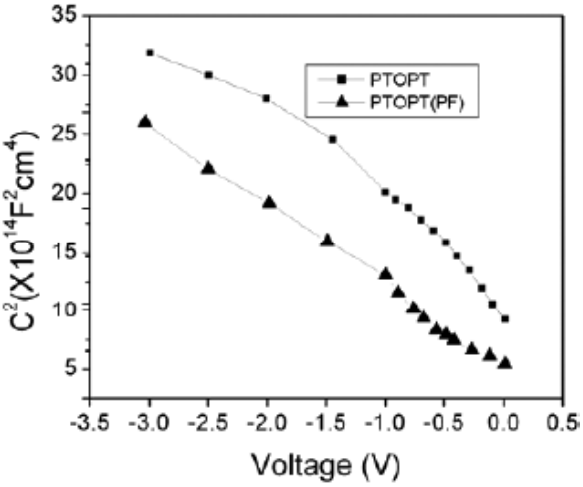

Fig. 4. *C-V* characteristics of Al/PTOPT/ITO with polymer (a) neutral (b) doped, data from [20].

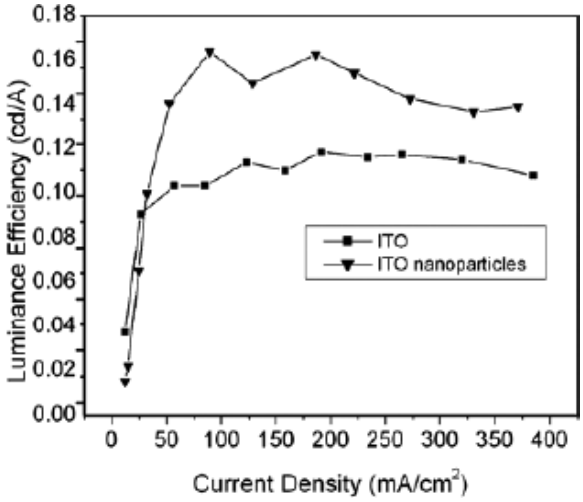

Fig. 5. Luminous Efficiency as a function of Current Density, data from [22].

temperatures close to the boiling point of glycerole, which is a direct contribution of increased conductivity and uniformity of the baked devices.

2.4. Polythiophene as emissive layer

Polythiophenes have been an active candidate for the electroluminescent materials in PLEDs [16]. Low PL quantum efficiency in the solid state (typically 1–3%) and poor EL performance of processable polythiophenes (PTs) have limited their application as emissive materials in PLEDs. The low PL efficiency of PTs could be attributed to the inter system crossing of excitons from the singlet to the triplet state and the intrinsic features of the electronic structure of PTs [17]. Ai-Lin Ding *et al.* [18] tried to explore the possibility of introducing some special functioning groups for the structural modification of polythiophenes. The extensive dealings on the design, synthesis, characterization and properties of a series of conjugated polymers, i.e., symmetrically substituted polymers, poly[(3-(4'-n-butylphenyl)-thiophene-2,5-diyl)(2,5-bis(decyloxy)-1,4-phenylene)[(4-(4'-n-butylphenyl)thiophene-2,5-diyl)] (PPTDOPPT), poly[(3-(4'-n- butylphenyl)thiophene-2,5-diyl)(2,5-bis(2-ethylhexyloxy)-1,4-phenylene) (4-(4'-n-butylphenyl)thiophene-2,5-diyl)] (PPTEHOPPT), and asymmetrically substituted polymer, poly[(3-(4'-n-butylphenyl)thiophene-2,5-diyl) (2-(2-ethylhexyloxy)-5-methoxy-1,4-phenylene) (4-(4'-n-butylphenyl)-thiophene-2,5-diyl)] (PPTEHMOPPT) sheds light into the effect of substitution on polymer structure and ultimately their physical, optical, and electrochemical properties. Characterization of PLEDs with calcium cathode (evaporated in 15 mm^2 active area), ITO anode and one of the above mentioned thiophene derivatives as luminescent material shows the improvement in quantum efficiency.

Having stability and ease of fabrication, Polythiophene and the family of its derivatives like poly [3-(4-octylphenyl)-2,2'-bithiophene], PTOPT, have attracted significant attention [19].

W. Bantikassegn [20], by using *Z-V* characterization augmented with the complex impedance and *C-V* analyses, explained the electronic properties of junctions between neutral or doped PTOPT and Al (Fig. 4). *J-V* characterization of the ITO/PTOPT (PFB) /Al (doped) and ITO/PTOPT/Al (undoped) indicates that turn on voltage of doped sample is half that of the undoped sample. Conductors form a rectifying barrier at the interface when the work function of the metal is smaller than that of the semiconductor. However, if the work functions are in the reverse order, the device gives an ohmic *J-V* characteristic (rather than rectifying).

2.5. Use of nano particles

Nanoparticles of ITO can provide transparent conducting films on plastic [21]. Use of ITO nano particles as anode material was first reported by Ali Cirpan and Frank E. Karasz [22]. The device exhibits a current density of 100 mA/cm^2, turn-ON voltage of 2.5V with a maximum luminance efficiency 0.135 and 0.09 cd/A. After a current density of 25

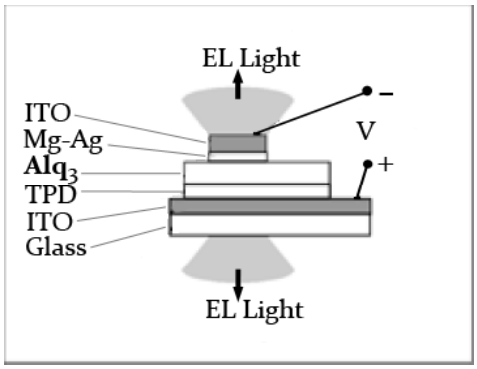

Fig. 6. A transparent organic light emitting device (TOLED) with five films [30].

mA/cm^2 the device with ITO nano particle has a considerable enhancement in luminous efficiency (Fig. 5). The electroluminescence spectra of conventional ITO and nanoparticle devices are consistent with exclusive emission from the chromophore layer.

Incorporation of nano particles into MEH-PPV results in improved photovoltaic efficiency. In such cases, CdSe [23] C_{60} [24] and TiO_2 [25,26] nanoparticles are used to make the polymer/nano particle composite films. The preparation of the solution is by first dispersing the TiO_2 nanoparticles in the solvent p-xylene and then added this mixture into MEH-PPV [26]. *J-V* characteristics and external quantum efficiency are found better and the most interesting observation is the radiance aging curve at constant voltage up to 80 hours, which shows a slower decay rate. The device exhibits an order in magnitude increase in current and luminance output and the improvement in performance was explained due to the change in device morphology caused by nano particles. A multilayer MEH-PPV device with an additional layer of carbon nanotube (CNT) exhibits a luminance of 3600 cd/m^2 at 5 V which is a significant achievement [27] with nanoblend.

2.6. Alternate cathodes

Replacing reactive cathodes by polymeric counterparts increases the electron injection and blocks the holes, thereby contributing to the overall stability of the device. Flux balance of charge carriers has been one of the prime approaches to improve the performance of passive driving displays [28]. The approaches for better balance include choice of metal cathode, modification of the interface, addition of electron/hole transport layer and modification of structure and morphology of emitting polymer.

The liquid cathodes are having a sharper metal-polymer interface due to high surface energy of the metals. The device performance due to this interface sharpness with liquid gallium cathode [29] showed a light emission two orders of magnitude than evaporated Al cathode device and external efficiency increased by an order of magnitude. The fabricated device used OC1C10-PPV as electroluminescent polymer, ITO anode and liquid Ga cathode. Despite the identical work functions of pure Al and Ga, there is a dramatic difference between the current density and light output of the two devices. Current density is more in liquid Ga devices; approximately by a factor of 10. The applied voltage for the same light emission is half for liquid Ga devices when compared with evaporated Al device. Neutral impact collision scattering spectroscopy and low energy ion scattering spectroscopy measurements are adapted for studying the interface property. The devices with liquid amalgam cathodes also exhibit a better performance when compared with their evaporated counterparts. It is worth noting that the enhanced performance was observed in experiments with high work function metals (evaporated Al and liquid Ga) and low work function metals (evaporated Ca and Ca amalgam).

2.7. Alternate design strategies

The Princeton University group had suggested a different configuration for PLED [30].The device (Fig. 6) is grown on a conducting substrate (basically glass), pre coated with a transparent indium tin oxide (ITO) thin film. On that, by evaporation in a vacuum is deposited a thicker layer of TPD (N,N'-diphenyl-N,N'-bis[3-methylphenyl]1-1'biphenyl-4,4'diamine). TPD is a "hole" conducting compound in which the absence of an electron acts as a carrier of a positive charge. The TPD layer is followed by a thick layer of the electron conducting and highly electroluminescent organic compound tris (8-hydroxyquinoline) aluminum (Alq3).So the device consists of five films laid down on glass. Sandwiched between top and bottom ITO films are three films: the hole injecting TPD layer and the electron injecting Mg-Ag layer and between them the Alq layer where holes and electrons recombine and give off light. Following the strategy of 'ITO on Top' proposed by Princeton group, D.Vaufrey *et al*. [31] fabricated top emitting organic light emitting diode by depositing ITO anode film onto polymer materials and electri-

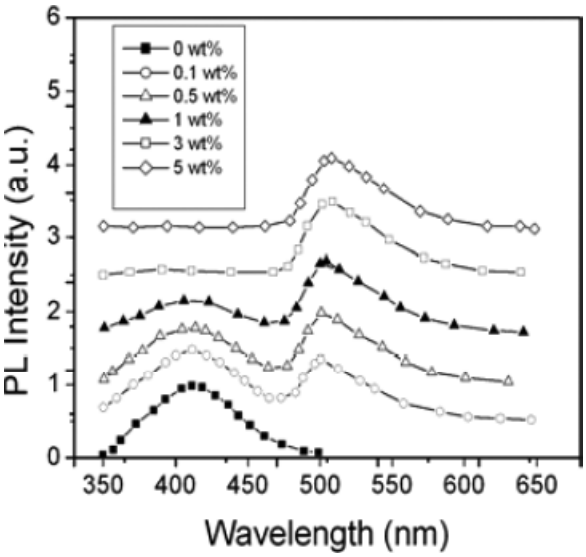

Fig. 7. PL Spectra of Blended film of PVK with different concentrations, data from [35].

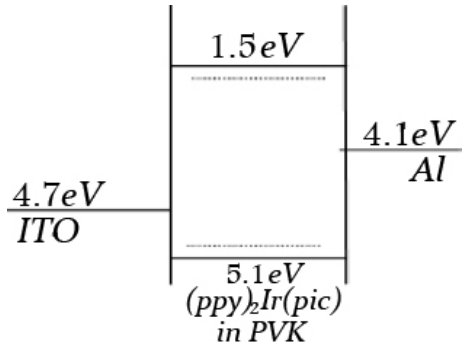

Fig. 8. Energy Level Diagram of OLED [35].

cal and optical behaviors of this inverted device have been characterized. Photo luminescence experiments depict the influence of plasma conditions for the deposition of ITO films. Study of Al/PVK/PEDOT/ sputtered ITO OLED structure is a novel approach in fabrication, bringing enhancements in performance along with it. The inverted organic photodiodes with highly conducting polymer anodes was demonstrated by Nyberg [32] Here the cathode of bismuth was vacuum evaporated first followed by a capping layer of C_{60}.

A semiconducting thiophene derivative (PEOPT) was spin coated on the cathode, followed by surface energy modification step and a subsequent spin coating of anode, a solution of glycerol and PEDOT-PSS. The device geometry was proven successful by I-V characterization of the device.

2.8. Devices with ISAM PPV films

The process steps in fabrication plays a vital role in the performance of the polymer light emitting device. Ionically Self Assembled Monolayer (ISAM) PPV films are recently developed class of materials which makes the structural and thickness control in sub nanometer regime [33]. The amount of deposited PPV can be controlled through pH and salt concentration.

The major step in process is dipping of a charged substrate alternately into poly cationic and poly anionic aqueous solutions at room temperature. Since the adsorption is based on the electrostatic attraction of interlayer charges, each layer is self-limiting in thickness and uniform at the molecular level. This occurs because the film molecules are free to adjust their positions to improve the overall packing since they are not covalently bound to the substrate. Sequential layers are rapidly fixed by drying at room temperature and pressure. Multilayer films several microns in thickness are easily fabricated by repeating the dipping process with no limit to the number of layers that can be deposited. The resulting pliable films are mechanically very robust and are only removed by vigorous scraping. The advantages afforded by molecular control on the sub nanometer level provide opportunities for dramatically enhanced photonic, electronic, and optoelectronic devices. The structure of the reported device is ITO/ISA/ (PPV/PMA)/Al (resistive evaporation). Small devices show large current density which is a remarkable breakthrough in performance studies of PLEDs.

2.9. Electro phosphorescent devices

The phosphorescent emission from osmium complex by singlets and triplets was successfully realized in late 90s. After that electrophosphorescent devices have been attracting greater attention as the goal was to achieve 100% internal efficiency. Past decade has witnessed to devices in which electrophosphorescent organic small molecules, including iridium (Ir), platinum (Pt),ruthenium (Ru), europium (Eu) and osmium (Os) complexes doped into wide band-gap small molecule host. Conjugated materials also have been used as host material since LEDs can be made by simple solution processing. Though high efficiency PLEDs can be fabricated by using polymer host material, decay in efficiency with increase in current density and the

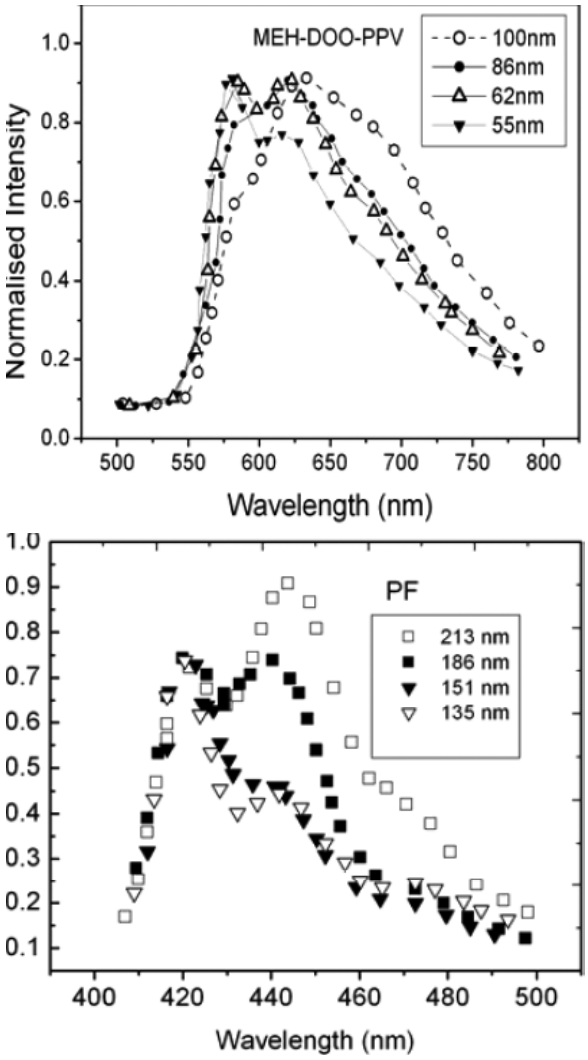

Fig. 9. Normalized Intensity of Single Layer MEH-PPV and PF Devices for different thicknesses, data from [36].

intrinsic instability in phase behavior of such blend systems during long-term storage and operation are the major problems on the way. By introducing phosphorescent complexes into the polymer main chain or onto side chain, these problems can be overcome. A review on the organometallic polymers as highly efficient emitters [34] explains the performance of devices with main chains with non conjugated polymers, conjugated polymers, organo metallic polymers and side chains with electro phosphorescent polymers.

Synthesis of new EL polymer namely bis (2-phenylpyridine- C^2, N') iridium (III) picolinate $(ppy)_2Ir(pic)$ with PVK is used as host polymer lead to the fabrication of single layer device whose emission is electrophopsphorescent in nature [35]. PL

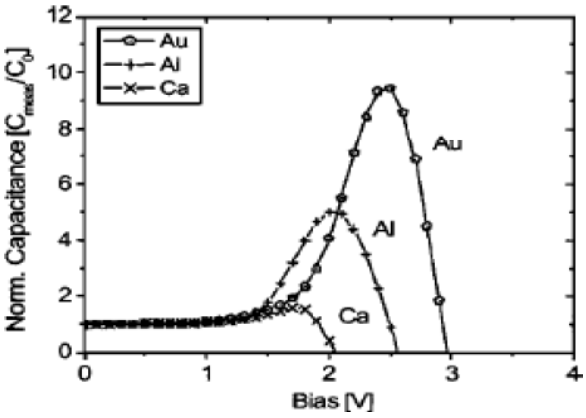

Fig. 10. Normalized Capacitance as a function of applied bias reported in [39].

spectra of blended film shown in Fig. 7. The energy transfer from PVK to $(ppy)_2Ir(pic)$ takes place with increase in the PL contribution of iridium complex on increasing its concentration. The energy transfer is complete at higher concentration of PVK (5%).

The band diagram of the device ITO/PEDOT/PVK: $(ppy)_2Ir(pic)$ /Al is as shown in Fig. 8. Though results on turn on voltage and quantum efficiency are not worthwhile to mention, the concept of a cyclometalated complex as PL layer shall be appreciated.

3. THICKNESS DEPENDENT CHANGES

Though there have been many studies on the changes in optical properties by varying the annealing conditions or changing the materials of cathode and EL polymer, one could come across few works on thickness dependent changes [36] in device performance. The observations on thickness related changes in optical properties of devices reveal some vital behavioral changes in the spectra. The studies on single layer devices with MEH-DOO-PPV and PF with 2% end cap as conducting polymers are conducted by J.M.Leger *et al.* [37]. The characterization of the PPV device with polymer layer thickness 55 ,62, 86, and 100 nm and that of PF device with thickness 135, 151, 186, and 213 nm indicate that lesser the thickness, earlier will be the peaks of normalized intensity (Fig. 9). The surface treatment of ITO results in better hole injection, effective quantum and power efficiencies, but when used with high work function metals, the same enhancement in power efficiency is not seen [38].

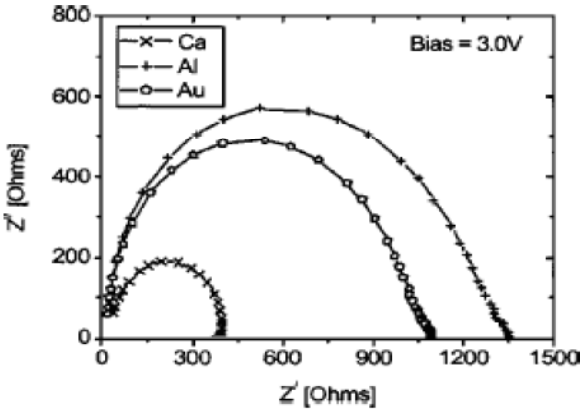

Fig. 11. Cole-Cole Plots with frequency as the implicit variable reported in [39].

4. C-V STUDIES OF PLED

Vishal Shrotriya and Yang Yanga [39] relate the behavior of *C–V* characteristics to the onset of majority and minority charge carrier injection into the active polymer layer from the electrodes. The structure of the devices was ITO/PEDOT: PSS/MEH-PPV/Cathode. Normalized capacitance (Fig. 10) measured is shown below for different electrodes used. At zero bias, the capacitance of the device is same as the geometrical capacitance $C = \varepsilon\varepsilon_0 A/d$, where ε, ε_0, $C = \varepsilon\varepsilon_0 A/d$, A, and d are relative dielectric constant of the polymer, permittivity of the free space, area of the device and the thickness of the polymer film respectively.

The constant capacitance of a PLED at reverse bias suggests that there exists a depleted region across the polymer film in the device, which in turn suggests that the device has a flat band structure in reverse bias. On applying a small forward bias, there is no apparent change in the value of capacitance, and it remains equal to C_0, the geometric capacitance, which is because of the dielectric properties of the polymer.This capacitance remains almost constant until a point where the majority charge injection begins from the anode. This majority carrier injection marks a sharp increase in the capacitance. On further increasing the bias, the minority charge injection occurs, which results in recombination of electrons and holes in the polymer and emission of photons and the amount of charge that is present in the polymer decreases significantly. This explains the decrease in the capacitance at a higher bias. This decrease in capacitance is not only because of the neutralization of trapped charges, but mainly because of the recombination

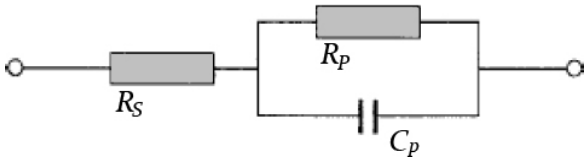

Fig. 12. Equivalent circuit of the device [40].

of electrons and holes, resulting in decrease in the amount of charges present in the polymer significantly. The above assumption is supported by the fact that the relative increase in the capacitance is more for the device with a higher work function metal as the cathode. While the onset voltage of majority charge injection from the anode is same for all the devices and independent of the kind of cathode selected, the minority injection from the cathode will take place at a much higher bias when the cathode has a higher work function. Until that point the charge accumulation in the polymer will keep on increasing, thereby increasing the capacitance. Also the bias at which capacitance starts decreasing is lowest for devices with Ca as the cathode, and highest for Au, which again can be explained by the fact that a higher bias is required for minority charge injection, in case of devices with higher work function cathode.

It has been reported that PLEDs behave like a pure capacitor for low applied bias, but for a dc bias higher than the energy gap of the polymer(2.1 eV for MEH–PPV in this case) the Z" vs Z' plot of PLED is a semicircle with a small tail at low frequencies, which is clear from the Fig. 11. The complex impedance of the device, Z can be expressed as $Z = Z' - Z''$, where Z' is the real part an Z'' is the imaginary part of the complex impedance.

The equivalent circuit (Fig. 12) gives more insight into the complex impedance of the device.

For a device having the structure of ITO/MEH-PPV/LiF/Al, the capacitance and conductance were measured in the frequency range of 10 Hz to 10 MHz for zero bias voltage to find the effect of LiF layer [40]. The effect of metal cap used along with cathode can be analyzed by admittance spectroscopy

$$Z = R_s + \frac{R_p - j\omega R_p^2 C_p}{1 + \omega^2 R_p^2 C_p^2}, \quad (1)$$

$$Z' = R_s + \frac{R_p}{1 + \omega^2 R_p^2 C_p^2}, \quad (2)$$

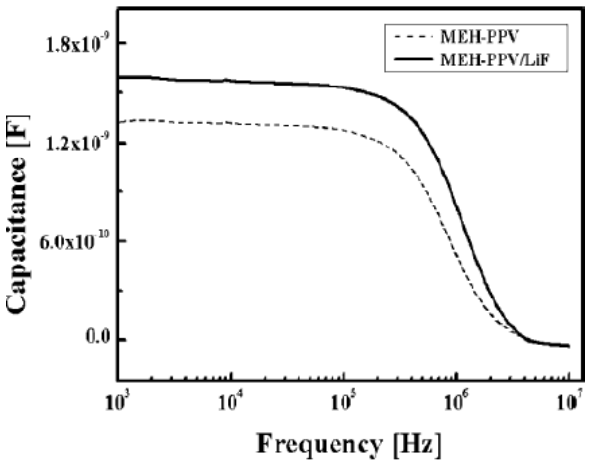

Fig. 13. Capacitance variation with frequency in the device with and without LiF as a buffer layer between cathode and organic interface, data from [40].

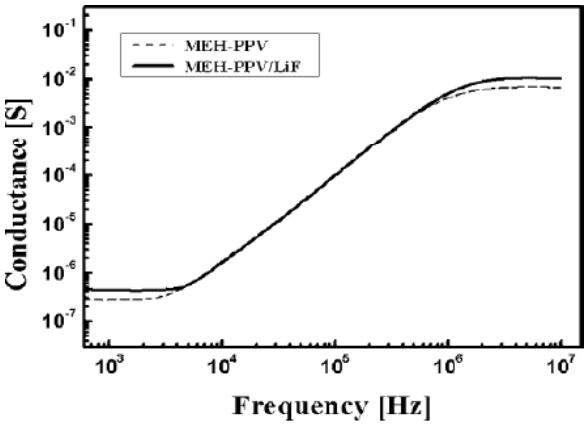

Fig. 14. Conductance variation with frequency in the device with and without LiF as a buffer layer between cathode and organic interface reported in [40].

$$Z'' = \frac{\omega R_p^2 C_p}{1+\omega^2 R_p^2 C_p^2}. \quad (3)$$

Fig. 13 shows the capacitance versus frequency (*C-F*) characteristics for the device with ITO-MEH-PPV-Al and ITO-MEH-PPV-LiF-Al structures. For the high frequency region, the values of capacitances with and without LiF layer are almost equal, but for the low frequency region, there is an increment in the capacitance with the introduction of the LiF layer, which is related to the enhancement of carrier injection and space charge formed by the injected carriers.

Fig. 14 shows that the conductance of the device increases for the low and high frequency region when the LiF layer is inserted into the cathode/organic interface, which is basically caused by carrier injection enhancement.

5. TRANSIENT ELECTROLUMINESCENCE STUDIES OF PLED

Transient EL has been attracting considerable interest for its potential application as a pulse light source and for high resolution displays. Upon the application of a rectangular voltage pulse to the OLED, one can study charge carrier kinetics and estimate charge carrier mobility from the temporal response of the EL [41]. A. Rihani *et al.* [42] elucidates the electrical excitation of PLED by means of fast pulse generator Tektronix PG2012 which permitted accurate control of repetition rate, rise and decay times. Single pulses were varied in time between 100 and 400 μs, and in magnitude between 2 V and 14 V. To avoid heating of the sample, all signals were with data cycle up to 50%. The EL response was detected using a PM Hamamatsu H5783 photomultiplier tube detector, and a 50 X external load resistance. Experimental setup for recording of the transient light, current, as well as the voltage across the sample, is shown in Fig.15. For a simultaneous recording of the three quantities we have used a fast digital Tektronix TDS 5034 oscilloscope. All measurements were carried out at room temperature in vacuum and all data were averaged at variables rates. The overall RC time constant of the measurement system was estimated to be much lower than 1 μsec. The EL spectrum of the device was measured with a Peltier cooled CCD camera coupled to a polychromator. Fig. 16 shows the EL spectrum of the device which is quite similar to any typical spectrum of a device based on the same material (MEHPPV), and there typical transient behaviors of EL and current in comparison with the applied rectangular voltage pulse (400 μs width and 9.75 V amplitude) are depicted.

In transient features the emission starts after a delay time t_d which is defined as the difference between the rising edge of the voltage pulse and the occurrence of the electroluminescence. An analytic solution for the EL slow rise in the electron dominated region can be obtained taken into account of some approximations based on the physical considerations as follows (i) for $t > t_d$, the hole density is independent of both time and space and it is not affected by the recombination; (ii) the hole density

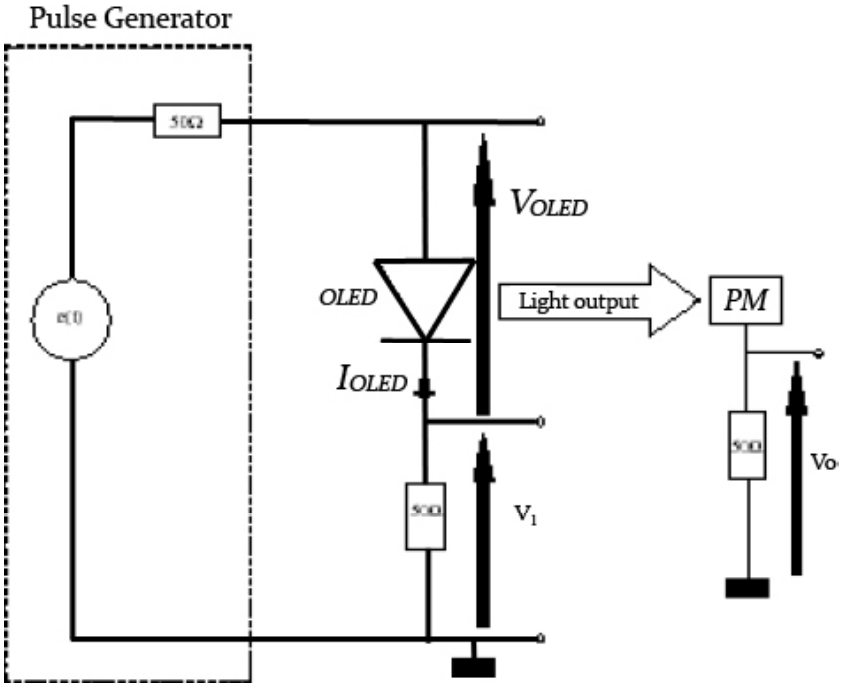

Fig. 15. Experimental set up for measuring transient EL [42].

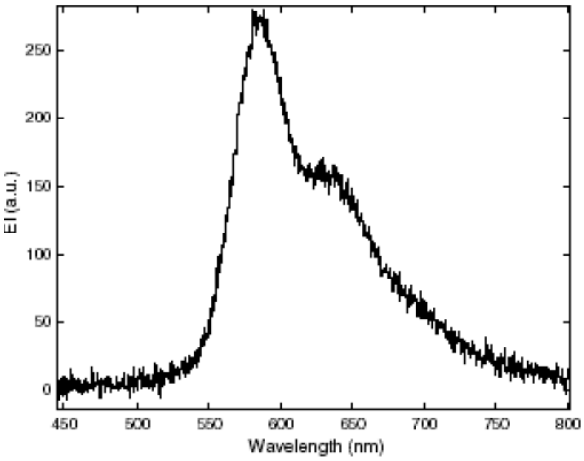

Fig. 16. EL Spectrum of the PLED, data from [42].

exceeds very much the electron one even at steady state (this can be achieved when the barrier for hole injection is small compared to the barrier for electron injection); (iii) in contrast to the EL decay mechanism after switching off. The bias which is due to charge trapping at the polymer/metal interface and controlled by diffusion of the fastest carriers (holes) in the polymer, the EL slow rise is due to Langevin recombination of free independent carriers and its mechanism is controlled by the slow motion of electrons under the effect of the applied electric field. Furthermore, since the EL signal is obtained when the applied voltage become relatively high (in general > 2 V), diffusion contribution to the current is negligible;(iv) at the range of applied voltage when the EL is obtained, it is assumed that the influence of traps is not important (all traps are filled).

A simple model for the transient slow rise of the EL turn-on in a single layer organic device presented is based on the continuity equations for carrier dynamics, as well as the expression of the recombination current [42]. It provides a simple means for estimating the free hole density at the equilibrium in the bulk after EL turn-on.

6. DEGRADATION PHENOMENA IN PLEDs

Though active researches are going on for stabilizing the device performance, degradation has been a vital impediment in commercialization of PLEDs. Degradation and failure of MEH-PPV devices have been a challenge before different groups who dream for long life organic display panels. Even in the absence of atmospheric oxygen and moisture, there occurs aromatic aldehyde formation and loss of conjugation which eventually lead to oxidative degradation. The formation of carbonyl species and loss of emissive efficiency due to fluorescence quenching effect [43] points to the physical mechanisms behind degradation. The loss of conjugation affects the device operation by reducing charge carrier mobility and hence increasing operating voltage. Changes in ITO IR spectrum suggests that ITO an-

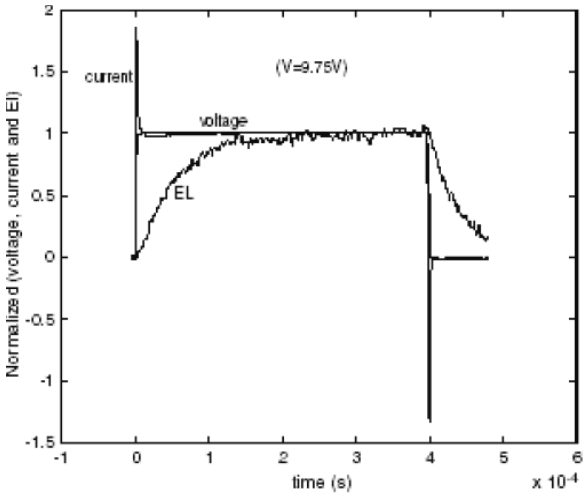

Fig. 17. Transient Behavior of the PLED, data from [42].

ode can serve as the source of oxygen for carbonyl formation. Experiments with polyaniline (PAni) between ITO and MEH-PPV in reducing the oxidative degradation were successfully reported by J.C. Scott *et al.* [44]. They have used the conventional spin casting technique, still the aging behavior of the device was found reduced by many orders.

The acidic nature of the ideal hole injection layer PEDOT-PSSA leads to etching of anode electrode, giving rise to unwanted free metallic ions. Further, PEDOT-PSSA suffers from UV and electron induced degradation and over oxidation which in turn can cause transition to insulating states [45]. Hence ample numbers of reasons are there to find improvements for PEDOT-PSSA as HIL. PAni-PSSA has been superior in many ways and different polymer counter ions are used for PEDOT and PAni. counter ion induced effects on electronic and morphological properties of the resulting films. The films made are [46]

1. PAni doped with Poly (styrene sulfonic acid)-PSSA
2. PAni doped with Poly (acrylamido-2-methyl-1-propanesulfonic acid)-PAA-MPSA
3. PAni-PAAMPSA blended with insulator polyacrylamide (PAM)
4. PEDOT where PAAMPSA is used as counter ions

In PAAMPSA doped polyaniline (which is actually a protonation) was normally made by oxidative polymerization of aniline. By using one of the above layers of films as HIL, PLEDs were fabricated with a configuration ITO (anode)/HIL (buffer layer)/Light Emitting Polymer/Ba (EIL)/Au (cathode). Photoelectron spectroscopy and UV absorption were used to study surface and bulk electronic properties. The behavior of the films with regard to intensity versus binding energy is characterized.

Table 2. Performance Comparison of four sets PLEDs under different baking conditions [46].

Material	Voltage (V)	Efficiency
PAni-PAAMPSA	3.3	7.5
PAni-PAAMPSA-PAM	4.6	8
PAni-PSSA	3.4	7.8
PEDOT-PAAMPSA	3.5	8

On device performance, turn on voltages and efficiencies of devices made using the listed HIL materials is given in Table 2. The work functions of PAni and PEDOT can be tuned over a large range by using polymeric counter ions with an improvement in performance.

Degradation in structural and optical properties of polyflourene based LEDs, by spectroscopic techniques with chemical and structural analysis was studied in late 90s [47]. Two modes of degradation are chemical route oxidation of polymer matrix leads to formation of aromatic ketone, which quenches the fluorescence and physical aggregation which leads to reduced intensity. Absorption and emission spectroscopy, infrared spectroscopy, and atomic force microscopy are the tools used in the experiments.

7. CONCLUSIONS

In this paper, we attempt to consolidate the important milestones in the development of polymer light emitting diodes by reviewing the major works on fabrication, characterization and analysis of the device. The experiments on the upgradation and modification of classical MEH-PPV structure, with more active layers and blends, are briefed in this review. Newer design strategies with ITO on top and upgraded electrodes have also been discussed. The way triplets effectively contribute to enhance the efficiency in electro phosphorescent devices, the phenomenal variations due to thickness variations of the emissive layer, impedance behaviour with *CV* studies and transient bahaviour of the device EL spectra points to the need of more collaborative efforts for overcoming the vital impediments in the commercialization of this most promising display device.

REFERENCES

[1] J.H. Burroughes, D.D.C. Bradley, A.R. Brown, R.N. Marks, K.Mackay, R.H. Friend, P.L. Burns and A.B. Holmes // *Nature* **347** (1990) 539.

[2] G. Gustafsson, G.M. Treacy, Y. Cao, F. Klavetter, N. Colaneriand and A.J. Heeger // *Synthetic Metals* ***55-57*** *(1993)* 4123.

[3] Y. Cao, G. Yu, C. Zhang, R. Menon and A.J. Heeger // *Synthetic Metals* **86** (1997) 2171.

[4] I.D. Parker // *J. Applied Physics* **75** (1994) 1656.

[5] D.Y. Kim, S.K. Lee, J.L. Kim, J.K. Kim, H. Lee, H.N. Cho, S.I. Hong and C.Y.Kim // *Synthetic Metals* **121** (2001) 1707.

[6] J. Birgerson, F.I.J. Janssen, A.W. Denier van der Gon, Y. Tsukahara, K. Kaeriyama and W.R. Salaneck //*Synthetic Metals* **132** (2002) 57.

[7] J. Bigerson, N. Johansson, A. Pohl, M. Logdlund, Y. Tsukahara, K. Kaeriyama and R. Salaneck // *Synthetic Metals* **122** (2001) 67.

[8] Andrew C. Grimsdale, Klaus Müllen // *Applied Polymer Science* **199** (2006) 1.

[9] Zhang-Lin Zhou, Xia Sheng, Lihua Zhao, Gary Gibson, Sity Lam, K. Nauka and James Brug // *Mater. Res. Soc. Symp. Proc. Vol. 1154 (*Materials Research Society, 2009)

[10] K.Chondroudis and D.B.Mitzi // *Chem.Mater.* **11**(1999) 3028.

[11] P.Cea, Y.Hua, C.Pearson, C.Wang, M.R.Bryce, M.C.Lopez and M.C.Petty // *Materials Science and Engineering C* **87-89** (2002).

[12] D.C. Tripathi, D.K.Sinha, C.K.Suman and Y.N.Mohapatra, In: *Proc. of ASID 2006,* (New Delhi, India, 2006).

[13] S. Ghosh, J. Rasmusson and O. Inganas // *Advance Materials* **10** (1998) 1097.

[14] A. Leshin, R. Kiebooms, R. Menon and A. Heeger // *Synthetic Metals* **90** (1997) 90.

[15] W.H.Kim, G.P.Kushto, H.Kim and Z.H.Karafi // *Journal of Polymeric Sciences:Part B; Polymer Physics* **41** (2003) 2522.

[16] Chengfeng Qiu, Zhiliang Xie, Haiying Chen, Ben Zhong Tang, Man Wong and Hoi-Sing kwok // *IEEE Journal of Selected Topics in Quantum Electronics* **10 1** (2004) 101.

[17] D.Belijonne, J.Cornil, R.H.Friend, R.A.J.Janssen and J.L.Bredas // *Journal of American Chemical Society* **118** (1996) 6453.

[18] Ai-Lin Ding, Jian Pei, Yee Hing Lai and Wei Huang // *Journal of Materials Chemistry* **11** (2001) 3082.

[19] M.R. Andersson, M. Berggren, O. Inganlis, G. Gustafsson, J.C.Gustafsson-Carlberg, D. Selse, T. Hjertberg and O. Wennerstrom // *Macromolecules* **28** (1995) 7525.

[20] W. Bantikassegn and O. Ingans // *Synthetic Metals* **87** (1997) 5.

[21] M.A. Aegerter and N. Al-Dahoudi // *Journal of Sol-Gel Science and Technology* ***27*** (2003) 81.

[22] Ali Cirpan and Frank E. Karasz // *Journal of Applied Polymer Science* **99** (2006) 3125.

[23] Jong Hyeok Park, So-Il Park, Tae-Ho Kim and O Ok Park // *Thin Solid Films* **515** (2007) 3085.

[24] K.W. Lee, K.H. Mo, J.W. Jang, N.K. Kim, W. Lee, I.-M. Kim and Cheol Eui Lee // *Current Applied Physics* **9** (2009) 1315.

[25] N.C.Greenham, Peng Xiaogang and A.P.Alivisatos // *Physical Review B* **54 17** (1996) 628.

[26] S.A.Carter, J.C.Scott and P.J.Brock // *Applied Physics Letters* 71 (9) (1997).

[27] Horng-Show Koo, Mi Chen, Hung-Wei Yu, Soon-Kap Kwon , Yong-Kyun Leea and Jin Jang // *Diamond & Related Materials* **16** (2007) 1162.

[28] Y.Z.Lee, X.W.Chen, S.A.Chen, P.K.Wei and W.S.Fann // *Jornal of American Chemical Society* **123** (2001) 2296.

[29] G.Anderson, H.P.Gommans, AW.Denier van der Gon and H.H.Brongersma // *Journal of Applied Physics* **93** (**6)** (2003).

[30] Zilan Shen, Paul E. Burrows, Vladimir Bulović, Stephen R. Forrest and M.E. Thompson // *Science* **276** (1997) 2009.

[31] David Vaufrey, Mohamed Ben Khalifa, Marie Paul Besland, Jacques Tardy, Cosmin Sandu, Marie-Genevieve Blanchin and Jean-Alain Roger // *Materials Science and Engineering C* **21** (2002) 265.

[32] T. Nyberg // *Synthetic Metals* **140 (2-3)** (2004) 281.

[33] D. Marciu, M. B. Miller, J. R. Heflin, M. A. Murray, A. L. Ritter, P. J. Neyman, W. Graupner, H. Wang, H. W. Gibson and R. M. Davis, In: *Proceedings of 3rd International Conference of Material Research Society on Smart Materials, Structures and Systems* (2008).

[34] Jiaxing Jiang, Wei Yang and Yong Cao // *Journal of Inorganic and Organometallic Polymers and Materials* **17 (1)** (2007) 37.
[35] Dipti Gupta, Sanjeev Singh, Monica Katyar, Deepak, Tanima Hazra, Avani Verma and Sundar S.Manoharan // *Materials and manufacturing processes* **21** (2006) 285.
[36] V.Bulovie, V.B.Khalfin, G.Gu and P.E.Burrows // *Physical Review B* **58** (1998) 3730.
[37] M.Leger, S.A.Carter, B.Rushtaller, H.G.Nothofer, U.Scherf, H.Tillman and H. Horhold // *Physical Review B* **68** (2003) 054209.
[38] Y.Shen, D.B.Jacobs, G.G.Malliaras, G.Koley, M.G.Spencer and A.Ioannidis // *Advance Materials* **13** (2001) 1234.
[39] Vishal Shotriya and Yang Yang // *Journal of Applied Physics* **97** (2005) 054504.
[40] H. M. Kim, U. Manna, K. S. Jang, J. Yi, Sunyoung Sohn, Keunhee Park and Donggeun Jung // *Mol. Cryst. Liq. Cryst.* **459** (2006) 11.
[41] J.W. Jang, C.E. Lee, D.W. Lee and J.-I. Jin // *Solid State Communications*. **130** (2004) 265.
[42] A.Rihani, L. Hassine, J.-L. Fave and H. Bouchriha // *Organic Electronics* **7** (2006) 1.
[43] M.Yan, L.J.Rothberg, F. Papadimitrikapoulos, M.E.Galvin and T.M.Miller // *Physical Review Letters* **73** (1994) 744.
[44] J.C.Scott, S.A.Carter, S.Karg and M.Angelopoulos // *Synthetic Metals* **87** (1997) 1197.
[45] A.W.Denier van der Gon, J.Birgerson, M.Fahlman and W.R.Salaneck // *Organic Electronics* **3** (2002) 111.
[46] Tengstedi, A.Crispin, H.Hsu, C.Zhang, I.D.Parker, W.R.Salaneck and M.Fahlman // *Organic Electronics* **6** (2005) 21.
[47] V.N.Bliznyuk, S.A.Carter, J.C.Scott, G.Klarner, R.D.Miller and D.C.Miller // *Macromolecules* **32** (1999) 361.